沼津工業高等専門学校研究報告
第54号，2020年1月

On the effective use of the multilevel algorithm in SU(2) lattice gauge theory

KOMA Yoshiaki*

We investigate the static quark-antiquark potential in SU(2) gauge theory by the lattice simulation with the multilevel algorithm, and examine how the numerical errors of the potential are controlled by the algorithm parameters. We find that one of the key parameters, the physical time extent of sublattices, is optimal when it is chosen to be around 0.37 fm, which is quite similar to that already observed in SU(3) lattice gauge theory.

Key Words: quark-antiquark potential, lattice gauge theory

I. INTRODUCTION

For the understanding of dynamics of quarks and gluons inside hadrons a quantum gauge field theory with non-Abelian SU(2) group symmetry, which we just call the SU(2) gauge theory, has often been investigated instead of realistic quantum chromodynamics (QCD) with SU(3) group symmetry [1]. This is because that the SU(2) group corresponds to a subgroup of SU(3), and is expected to describe some of essential features of QCD. Numerical investigation is usually needed for the understanding of nonperturbative properties of the theory, and a powerful method for this purpose is to define the theory on a hypercubic discrete lattice, and then compute its partition function by a Monte-Carlo method using supercomputers. We call this method the lattice simulation.

The lattice simulations generally provide us with expectation values of physical quantities. The static quark-antiquark potential (a variation of the potential energy as a function of the distance between a quark and an antiquark) is one of the typical quantities computed nonperturbatively by the lattice simulation. Once the potential is provided, it is possible to investigate the bound state of a quark and an antiquark by solving the Schrödinger equation, which are then compared to meson spectra observed by high-energy accelerator experiments [2]. The functional form of the potential is also used to understand the nontrivial vacuum structure.

However, since the expectation values are generally given by statistical averages of operators constructed with a sequential chain of independent vacuum configurations, they are accompanied by numerical errors. That is to say, one always faces problem of accuracy of the numerical result. Therefore, it usually takes longer computer time to obtain solid results. Even the quark-antiquark potential, which is a rather well-known quantity, has still room for improvement on the numerical accuracy.

In this report, we present some of preliminary results on the quark-antiquark potential in SU(2) gauge theory obtained by the lattice simulation with the multilevel algorithm [3, 4]. We compute the Polyakov loop correlation function (PLCF), which is defined by a pair of spatially separated Polyakov and anti-Polyakov loops, and extract the ground state potential straightforwardly. We then examine how the numerical errors of the potential are controlled by the algorithm parameters, aiming to find an optimal set of parameters to achieve efficient error reduction.

II. NUMERICAL PROCEDURES

We consider SU(2) gauge theory in four dimensions with lattice volume $L^3\times T$ and lattice spacing a, and impose periodic boundary conditions in all space-time directions. We use the standard Wilson gauge action composed of link variables $U_\mu(x)\in\mathrm{SU}(2)$ as

$$S=\beta\sum_{x,\mu<\nu}\{1-\frac{1}{2}\mathrm{ReTr}[U_\mu(x)U_\nu(x+\hat{\mu})U_\mu^\dagger(x+\hat{\nu})U_\nu^\dagger(x)]\}. \quad (1)$$

Basic building blocks of the PLCF are two-link correlators defined by

$$\mathbb{T}(x_0,\vec{x}_1,\vec{x}_2)_{\alpha\beta\gamma\delta}\equiv U_0(x_0,\vec{x}_1)_{\alpha\beta}U_0^\dagger(x_0,\vec{x}_2)_{\gamma\delta}, \quad (2)$$

where the Greek indices of $U_0(x)$ label the component of a 2×2 complex matrix for the SU(2) group.

*Division of Liberal Arts / Physics group

A two-link correlator is nothing but the direct product of two temporal link variables separated by a distance $r = |\vec{x}_1 - \vec{x}_2|$. The two-link correlator acts on a color state in the $\mathbf{2} \otimes \bar{\mathbf{2}}$ representation of the SU(2) group $|n; \vec{x}_1, \vec{x}_2\rangle_{\alpha\beta}$ with the principal quantum number n, which satisfies $\mathbb{T}(x_0, \vec{x}_1, \vec{x}_2)_{\alpha\lambda\gamma\epsilon}|n; \vec{x}_1, \vec{x}_2\rangle_{\alpha\gamma} = e^{-E_n(r)a}|n; \vec{x}_1, \vec{x}_2\rangle_{\lambda\epsilon}$, where $E_n(r)$ (> 0) corresponds to the energy. The multiplication law of two-link correlators between two neighboring time slices x_0 and $x_0 + a$ is

$$\{\mathbb{T}(x_0, \vec{x}_1, \vec{x}_2)\mathbb{T}(x_0 + a, \vec{x}_1, \vec{x}_2)\}_{\alpha\beta\gamma\delta} = \mathbb{T}(x_0, \vec{x}_1, \vec{x}_2)_{\alpha\lambda\gamma\epsilon}\mathbb{T}(x_0 + a, \vec{x}_1, \vec{x}_2)_{\lambda\beta\epsilon\delta} \ , \quad (3)$$

where the repeated Greek indices λ and ϵ are to be summed over from 1 to 2. The PLCF is finally constructed as

$$\mathrm{Tr}P(\vec{x}_1)\mathrm{Tr}P(\vec{x}_2)^* = \{\mathbb{T}(0, \vec{x}_1, \vec{x}_2)\mathbb{T}(a, \vec{x}_1, \vec{x}_2)\cdots\mathbb{T}(T-a, \vec{x}_1, \vec{x}_2)\}_{\alpha\alpha\gamma\gamma} \ . \quad (4)$$

Based on the transfer matrix formalism, the expectation value of the PLCF is evaluated formally by inserting the complete set of eigenstates at all time slices $x_0 = 0, a, ..., T - a$, which leads to a relation

$$\langle \mathrm{Tr}P(\vec{x}_1)\mathrm{Tr}P(\vec{x}_2)^* \rangle = \sum_{n=0}^{\infty} e^{-E_n(r)T} \ . \quad (5)$$

The ground state potential, $V(r) \equiv E_0(r)$, is then extracted by

$$V(r) = -\frac{1}{T} \ln\langle \mathrm{Tr}P(\vec{x}_1)\mathrm{Tr}P(\vec{x}_2)^* \rangle + O(e^{-(\Delta E)T}). \quad (6)$$

The systematic error term of $O(e^{-(\Delta E)T})$ is associated with the excited states, which is always negligible at zero temperature as the size of T is usually taken large enough. Once the potential is computed accurately, it is also possible to investigate the force from the derivative (difference) as

$$F(r) = \frac{dV(r)}{dr} = \frac{V(r + a) - V(r - a)}{2a} \ . \quad (7)$$

A numerical problem is that it is impossible to compute the PLCF in Eq. (5) accurately within the ordinary lattice simulations as the expectation values are extremely small at long distances, which are easily obscured by the statistical noise. We then employ the multilevel algorithm, which allows us to overcome the problem on the smallness of the PLCF.

The idea of the algorithm is to compute a correlation function from the product of sublattice averages of its components, where a sublattice is defined by dividing the lattice volume into several layers along the time direction. During the computation of sublattice averages, spatial links at the sublattice boundaries are fixed. The computation of correlation functions in this way is supported by the transfer matrix formalism. In order to use the multilevel algorithm efficiently, however, the number of time slices in a sublattice N_{tsl} and the number of internal updates N_{iupd} must be chosen appropriately depending on the gauge coupling β in Eq. (1).

III. NUMERICAL RESULTS

Our previous study of SU(3) lattice gauge theory showed that an optimal choice of aN_{tsl} was around 0.37 fm (1 [fm] $= 10^{-15}$ [m]) [5, 6]. By taking into account this observation, we have performed an extensive test of the algorithm parameters in SU(2) lattice gauge theory. In this report, we present a part of the results at $\beta = 2.45$ and 2.55 for $N_{\mathrm{tsl}} = 4$ (see, Table I), and demonstrate how the choice of parameters affects the effectiveness of the algorithm.

In Figs. 1 – 4, we show numerical results of the history of the PLCF, the potential, the force, and the relative error of the potential at $\beta = 2.45$ (left) and $\beta = 2.55$ (right), respectively. While we only plot the on-axis data for the PLCF such that the relative position vector between a quark and an antiquark is $\vec{r}/a = (n, 0, 0)$ with $n = 1, 2, 3...$, we plot both the on-axis and the off-axis data such as $\vec{r}/a = (n, n, 0)$, $\vec{r}/a = (n, n, n)$, $\vec{r}/a = (2n, n, 0)$ for other results (permutation of the x, y, and z axes is also taken into ac-

TABLE I: The list of simulation parameters. The Sommer scale r_0 is determined so as to satisfy $r_0^2 F(r_0) = 1.65$, where r_0 is often regarded as 0.50 fm.

β	L^3T	N_{tsl}	N_{iupd}	N_{cnf}	r_0/a	a [fm]	aN_{tsl} [fm]
2.45	32^4	4	50000	20	5.37	0.0931	0.3724
2.55	32^4	4	50000	20	7.476	0.0669	0.2676

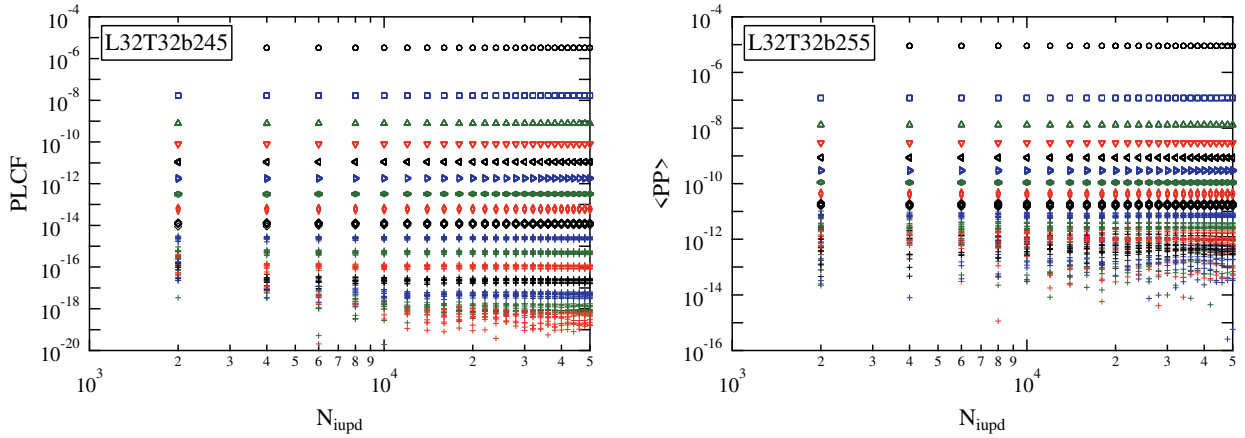

FIG. 1: The history of the PLCF as a function of $N_{\rm iupd}$ at $\beta = 2.45$ (left) and $\beta = 2.55$ (right) for all $N_{\rm cnf} = 20$ configurations. The bunch of plateau from upper to lower corresponds to the quark-antiquark distance $r/a = 1, 2, ...$, respectively, where only the on-axis data are plotted.

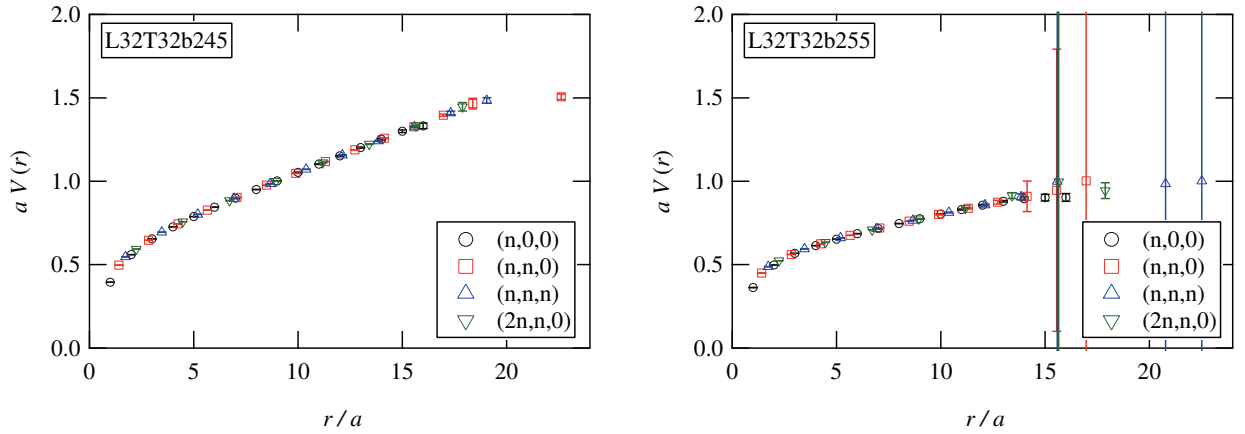

FIG. 2: The potential as a function of the quark-antiquark distance r/a at $\beta = 2.45$ (left) and $\beta = 2.55$ (right), where not only the on-axis data but also the off-axis data are plotted.

count to increase the statistics). The numerical errors in Figs. 2 and 3 are evaluated by the single-elimination jackknife method with $N_{\rm cnf} = 20$ configurations.

Fig. 1 exhibits that it is possible to compute extremely small expectation values by increasing the $N_{\rm iupd}$ only when the physical temporal length $aN_{\rm tsl}$ is optimally chosen. For the result at $\beta = 2.45$ the order of magnitude of the smallest plateau is of $O(10^{-18})$. For the result at $\beta = 2.55$, on the other hand, the smallest plateau of the PLCF is of $O(10^{-14})$ and it seems difficult to obtain further small expectation values even if the $N_{\rm iupd}$ is increased. Note that the value of $aN_{\rm tsl}$ at $\beta = 2.55$ is about 30% smaller than that at $\beta = 2.45$. The potential in Fig. 2 is computed by using the values of PLCF at $N_{\rm iupd} = 50000$. The result is clean up to $r/a \sim 18$ at $\beta = 2.45$, while up to $r/a \sim 14$ at $\beta = 2.55$. For the force the result at $\beta = 2.45$ is clearly better than that at $\beta = 2.55$ up to long distances as shown in Fig. 3. This tendency is of course reasonable since the force is computed from the difference of the potential. The scatter plot of the relative error of the potential in Fig. 4 explicitly demonstrates the effectiveness of the multilevel algorithm on the choice of algorithm parameters. The effect of the error reduction is better at $\beta = 2.45$ than that at $\beta = 2.55$, especially at long distances.

IV. SUMMARY

We have investigated the static quark-antiquark potential in SU(2) gauge theory by using the lattice simulation with the multilevel algorithm [3, 4], and

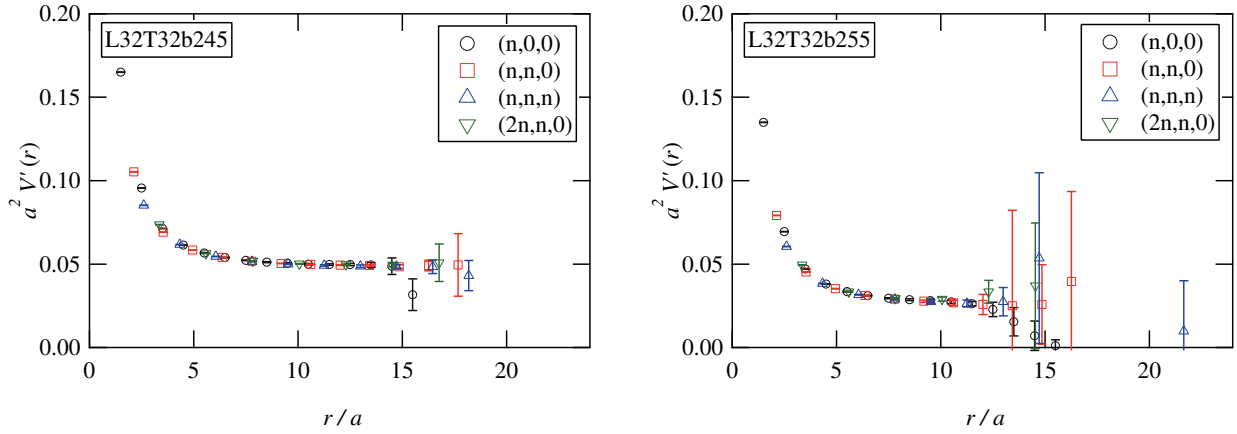

FIG. 3: The force as a function of the quark-antiquark distance r/a at $\beta = 2.45$ (left) and $\beta = 2.55$ (right), where not only the on-axis data but also the off-axis data are plotted.

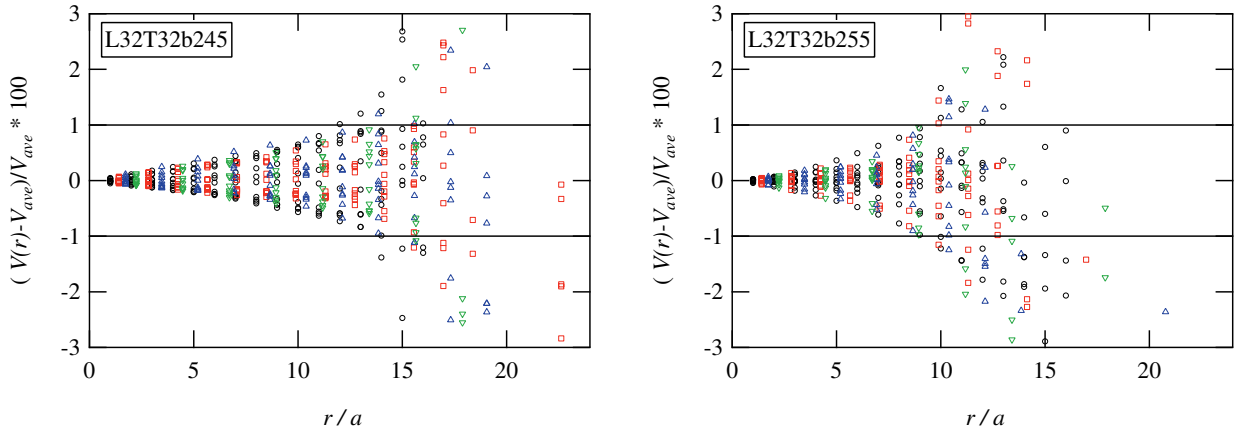

FIG. 4: The relative error of the potential (the relative differences of the potentials between each of $N_{\rm cnf} = 20$ configurations and their average) as a function of the quark-antiquark distance r/a at $\beta = 2.45$ (left) and $\beta = 2.55$ (right), where not only the on-axis data but also the off-axis data are plotted.

have examined how the numerical errors of the potential are controlled by the algorithm parameters, where the key parameters are the number of time slices in a sublattice $N_{\rm tsl}$ and the number of internal updates $N_{\rm iupd}$. We have compared the results of the PLCF, the static potential, the force, and the relative error of the potential at $\beta = 2.45$ and 2.55 for $N_{\rm tsl} = 4$, and have found that $N_{\rm tsl} = 4$ is suitable for $\beta = 2.45$ and unsuitable for $\beta = 2.55$. These results suggest that the optimal condition $aN_{\rm tsl} \simeq 0.37\,{\rm fm}$ [5, 6], which is observed in SU(3) lattice gauge theory, seems to hold also in SU(2) lattice gauge theory.

The author is grateful to M. Koma for fruitful collaboration. The lattice simulations have been performed on the NEC SX-ACE at Research Center for Nuclear Physics (RCNP) and Cybermedia center, Osaka University.

[1] W. Greiner and A. Schäfer, Quantum chromodynamics, Springer-Verelag, Berlin and Heidelberg, 1994.
[2] M. Tanabashi et al. (Particle Data Group), *Phys. Rev. D* **98** (2018) 030001.
[3] M. Lüscher and P. Weisz, *JHEP* **0109** (2001) 010.
[4] M. Lüscher and P. Weisz, *JHEP* **0207** (2002) 049.
[5] Y. Koma, M. Koma, and H. Wittig, *Phys. Rev. Lett.* **97** (2006) 122003.
[6] Y. Koma and M. Koma, *Nucl. Phys.* **B769** (2007) 79–107.